

Construction of Ni/Ni₃N Heterojunction as Lithium Polysulfides Reversible Micro-Reaction Centers

Tingjiao Xiao^a, Fengjin Yi^a, He Wang^a, Mingzhi Yang^a, Weiliang Liu^a, Manman

Ren^{a,*}, Xu Zhang^{b,*}, Zhen Zhou^b

^a School of Materials Science and Engineering, Qilu University of Technology (Shandong Academy of Sciences), Jinan 250353, PR China

^b Engineering Research Center of Advanced Functional Material Manufacturing of Ministry of Education, School of Chemical Engineering, Zhengzhou University, Zhengzhou 450001, P. R. China.

Experimental section

Preparation of Materials

Hollow carbon nanotubes (CNT) were firstly synthesized using the method which has been reported in the previous work¹. Next, 15 mL of ethanol, 0.2 g of CNT and 0.4 g of NiCl₂·6H₂O mixed uniformly by ultrasonication, and then the mixture was dried at 50°C. The obtained powder was calcined at 600 °C for 3 h in a pure ammonia atmosphere to obtain the Ni/Ni₃N-CNT, and calcined at 500°C for 3 h to obtain the Ni₃N-CNT.

The Ni/Ni₃N-CNT/S electrode materials were obtained through a typical melt-diffusion approach. Sulfur powder was well-mixed with Ni/Ni₃N-CNT with a weight ratio of 6:4. Then the mixture was heated at 155°C for 12 h in an argon atmosphere. The Ni₃N-CNT/S was also prepared through the same procedure.

Adsorption test

The first step in this section is to prepare the Li_2S_6 solution (5 mM). Li_2S and S were firstly dissolved in a solution of DME/DOL ($v/v = 1:1$) with a molar ratio of 1:5, followed by continuous stirring at 60°C for 18 h. Next, Ni/ Ni_3N -CNT and Ni_3N -CNT with the same weight (20 mg) were added to the Li_2S_6 solution (2 mL), respectively. Finally, the mixed solutions were vigorously shaken for 2 min and then rested at room temperature for 3 h.^{2,3}

Electrochemical measurements of LSBs

The active materials (Ni/ Ni_3N -CNT/S and Ni_3N -CNT/S), polyvinylidene fluoride (PVDF), and acetylene black with the weight ratio of 7:1:2 was dispersed in NMP to form a uniform slurry. Then the slurry was coated onto an Al foil and dried at 50°C for 12 h under vacuum. The diameter of the electrode was 1.2 cm, and the sulfur loading was 1.2 mg cm^{-2} in long cycle performance at 1 C and 5 C, the sulfur loading was 5 mg cm^{-2} in Figure 7b.

Electrochemical performances were tested in a standard CR2032 simulated battery with Li foil and PP as the anode and separator, respectively. Under normal conditions, the electrolyte is a solution of 1.0 M LiTFSI and 1.0 % LiNO_3 dissolved in DME/DOL ($v/v = 1:1$). The electrolyte dosage was accurately controlled with an electrolyte/sulfur ratio $\approx 50\text{ }\mu\text{L mg}^{-1}$. Galvanostatic charge/discharge measurements were performed on a Neware battery testing system in a potential window of 1.7-2.8 V. CV were conducted on a CHI760E electrochemical workstation at different scan rates in the potential range of 1.7-2.8 V. EIS spectra were obtained on a CHI760E electrochemical workstation, the frequency ranged from 100 kHz to 0.01 Hz and the amplitude was 5 mV.

Material Characterization

Morphological characterization of the prepared samples was measured using scanning electron microscope (SEM, Hitachi S-4800), Transmission electron microscope (TEM), and high-resolution TEM (Tecnai G2F30S-Twin). X-ray diffractometer (XRD) tests of the samples were conducted by using Cu K α radiation (Shimadzu XRD-6100AS). Nitrogen adsorption/desorption isotherms and Brunauer-Emmett-Teller surface area were gained with a Micromeritics Gemini V2380 analyzer operating at 77 K. X-ray photoelectron spectroscopy (XPS) analysis was obtained using an ESCALAB250 spectrometer with Mg K α radiation as the excitation source. TGA (METTLER) was conducted in air at a heating rate of 10 °C min⁻¹.

Theoretical Calculation

Here the density functional theory (DFT) calculations were performed based on plane-wave technique as implemented in Vienna ab initio simulation package (VASP).⁴ The projector augmented wave (PAW) approach was adopted to describe the ion-electron interaction.⁵ The generalized gradient approximation (GGA) in the form of functional of Perdew, Burke, and Ernzerhof (PBE) was used to describe the exchange-correlation energy.⁶ An energy cutoff of 450 eV was used for the plane wave-basis set. The revised Perdew-Burke-Ernzerhof (RPBE) functional was employed to describe the adsorption of sulfides on metal surfaces.⁷ To avoid the artificial interactions, a vacuum space with at least 20 Å was inserted along *z* direction. Considering the crystal lattice match between Ni and Ni₃N, the model of (001) surface was built in this work. A Monkhorst-Pack *k*-point mesh of 3×3×1 was used.⁸ For the surface model, the lower

two atomic layers of the slabs were fixed during optimization while other atoms were fully relaxed.

When the polysulfides including (especially S₈ and Li₂S₈) adsorbed on the metal surface, these molecules would be decomposed and therefore the reaction energy of the discharge process from Li₂S₆ to Li₂S on the metal surfaces was computed based on the reaction sequence of *Li₂S₆ → *Li₂S₄ → *Li₂S₂ → *Li₂S. The corresponding reaction energy was calculated by:

$$E_{*Li_2S_4} + \frac{1}{4}E_{S_8} - E_{*Li_2S_6}$$

$$E_{*Li_2S_2} + \frac{1}{4}E_{S_8} - E_{*Li_2S_4}$$

$$E_{*Li_2S} + \frac{1}{4}E_{S_8} - E_{*Li_2S_2}$$

in which $E_{*Li_2S_x}$ is the energy of the Li₂S_x molecule adsorbed on catalysts, E_{Li} is the energy of Li atom in lithium metal and E_{S_8} is the energy of isolated S₈. The adsorption energy (E_{ads}) was computed by the equation:

$$E_{ads} = E_{tot} - E_{Li_xS_y} - E_{cat}$$

where E_{tot} , $E_{Li_xS_y}$ and E_{cat} represent the total energy of the complex of the adsorbates (Li_xS_y molecules) and the catalysts, the isolated Li_xS_y molecules and the catalysts, respectively.

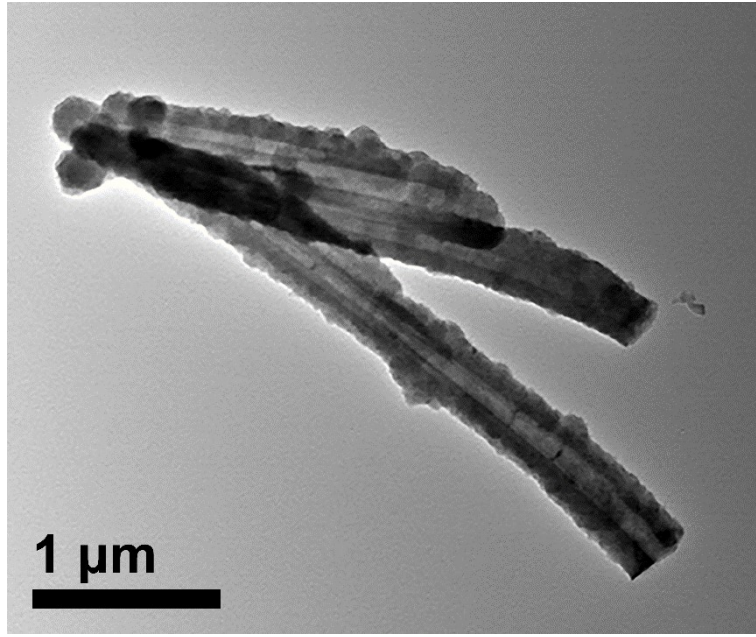


Figure S1. TEM images of the CNT.

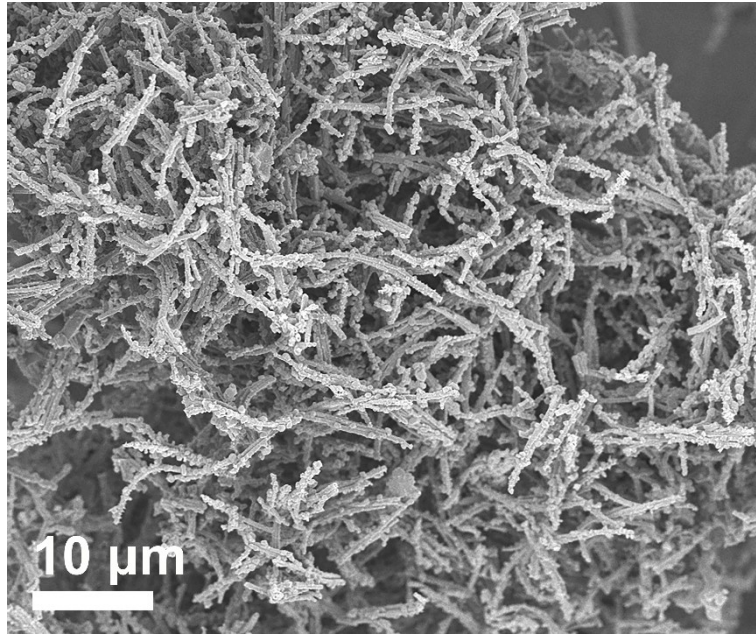


Figure S2. SEM images of the Ni/Ni₃N-CNT.

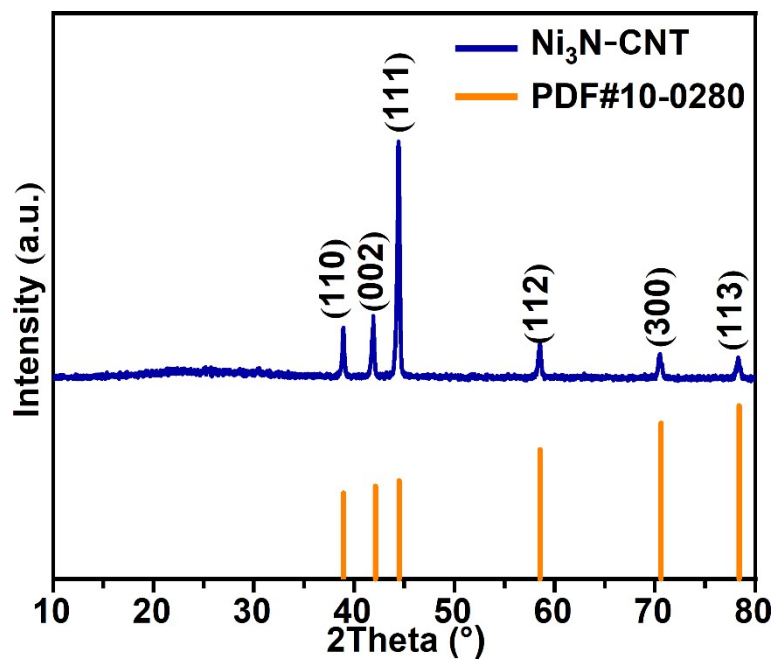


Figure S3. XRD patterns of the Ni₃N-CNT.

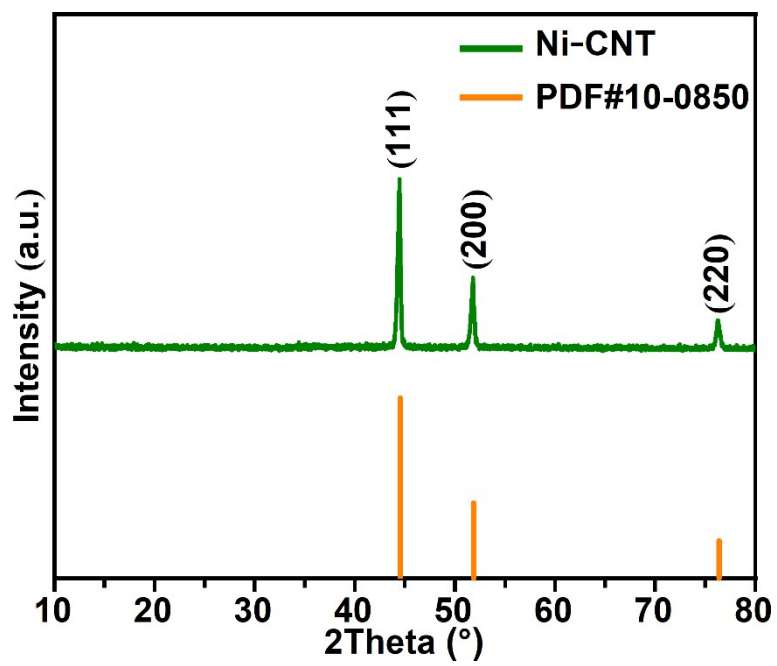


Figure S4. XRD patterns of the Ni-CNT.

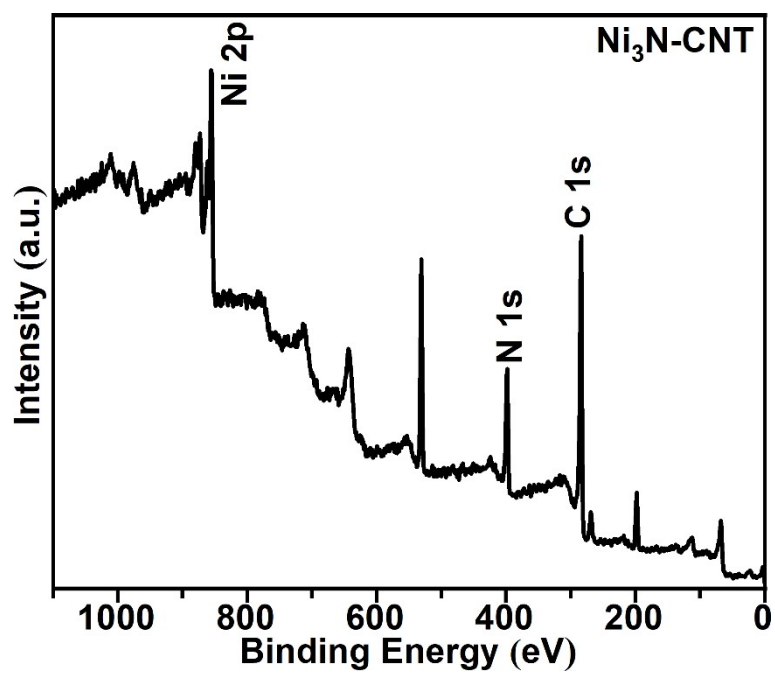


Figure S5. XPS survey spectrum of the Ni₃N-CNT

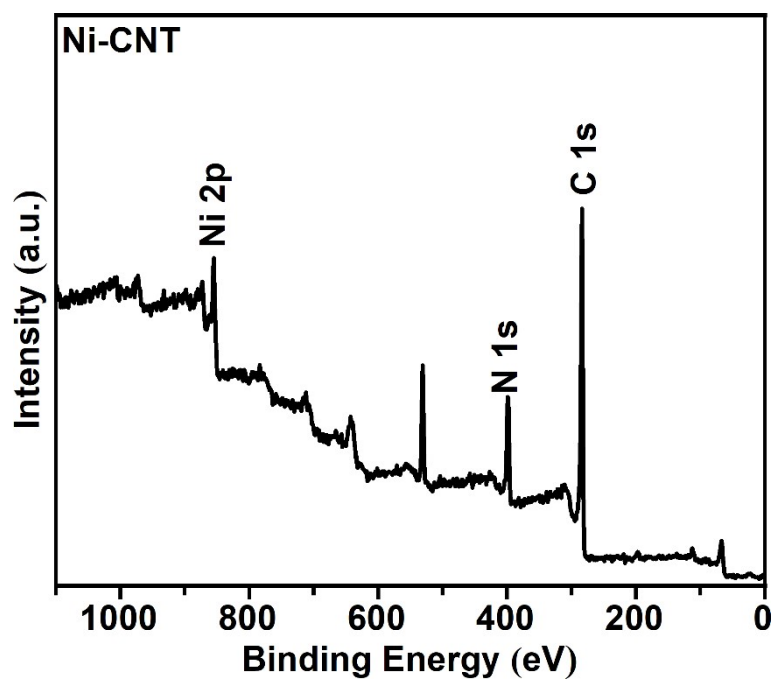


Figure S6. XPS survey spectrum of the Ni-CNT.

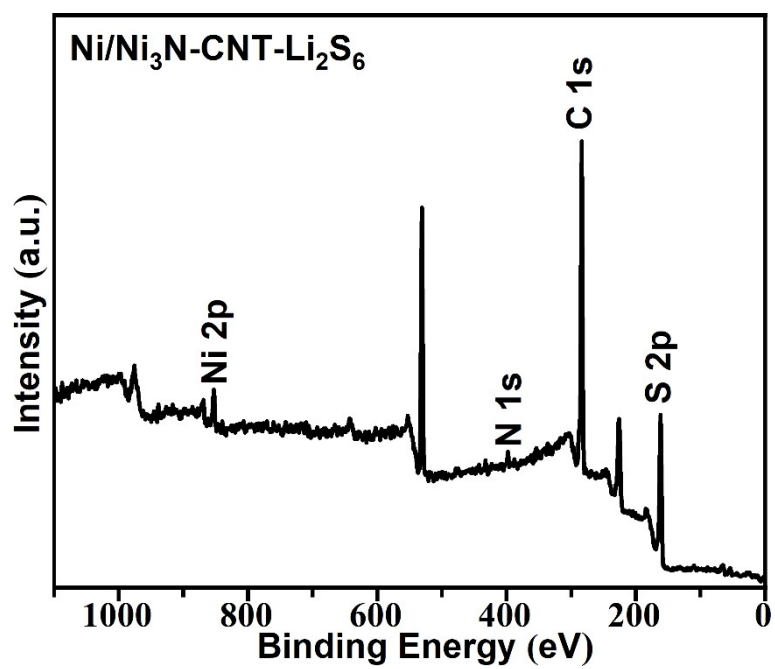


Figure S7. XPS survey spectrum of the Ni/Ni₃N-CNT-Li₂S₆.

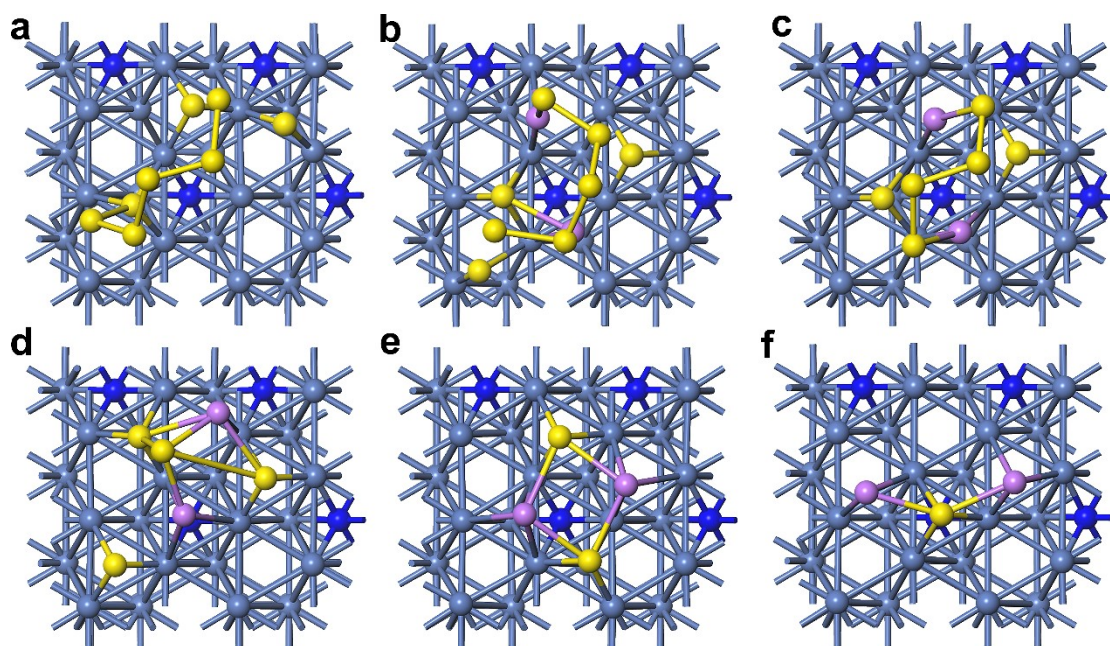


Figure S8. Optimized structures of S₈ (a), Li₂S₈ (b), Li₂S₆ (c), Li₂S₄ (d), Li₂S₂ (e) and Li₂S (f) on the Ni/Ni₃N surface. Yellow, purple balls represent S, Li atoms, respectively.

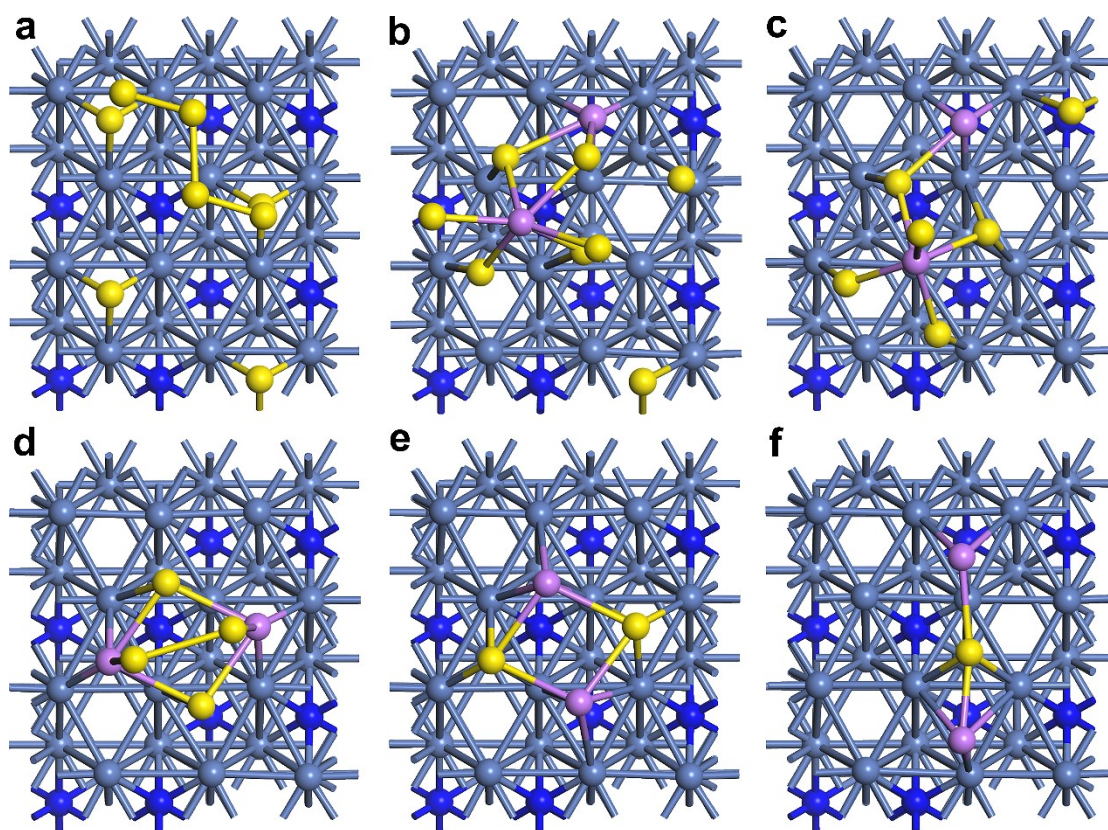


Figure S9. Optimized structures of S_8 (a), Li_2S_8 (b), Li_2S_6 (c), Li_2S_4 (d), Li_2S_2 (e) and Li_2S (f) on the Ni_3N surface. Yellow, purple balls represent S, Li atoms, respectively.

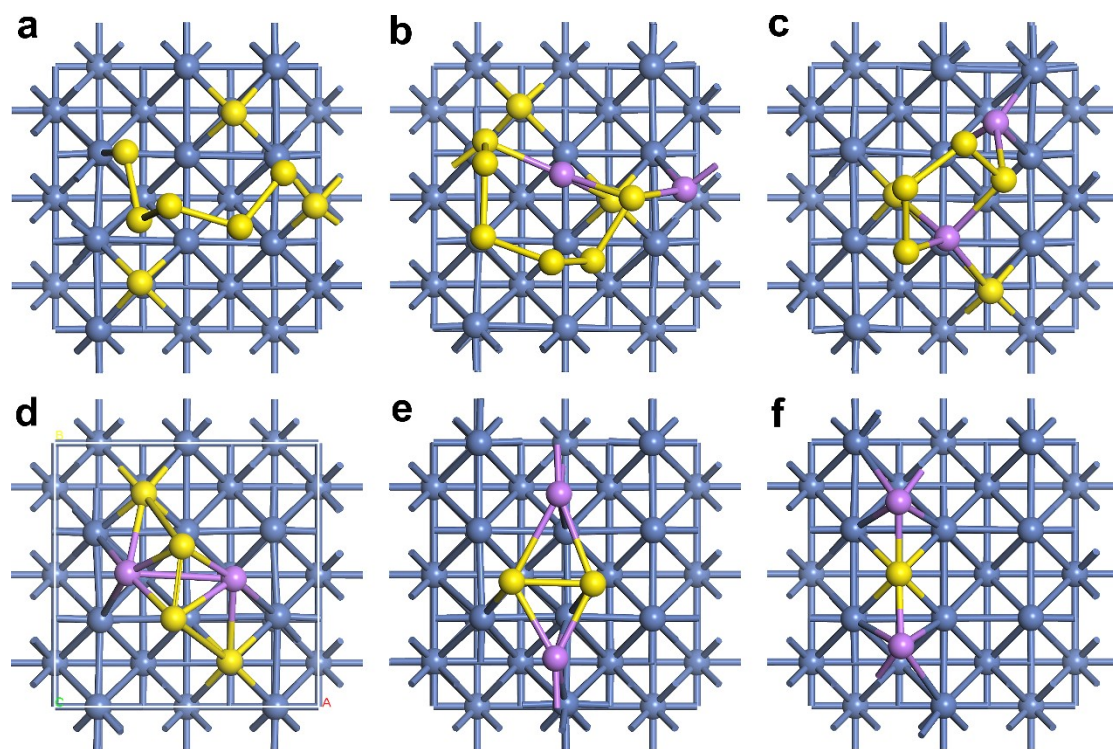


Figure S10. Optimized structures of S₈ (a), Li₂S₈ (b), Li₂S₆ (c), Li₂S₄ (d), Li₂S₂ (e) and Li₂S (f) on Ni the surface. Yellow, purple balls represent S, Li atoms, respectively.

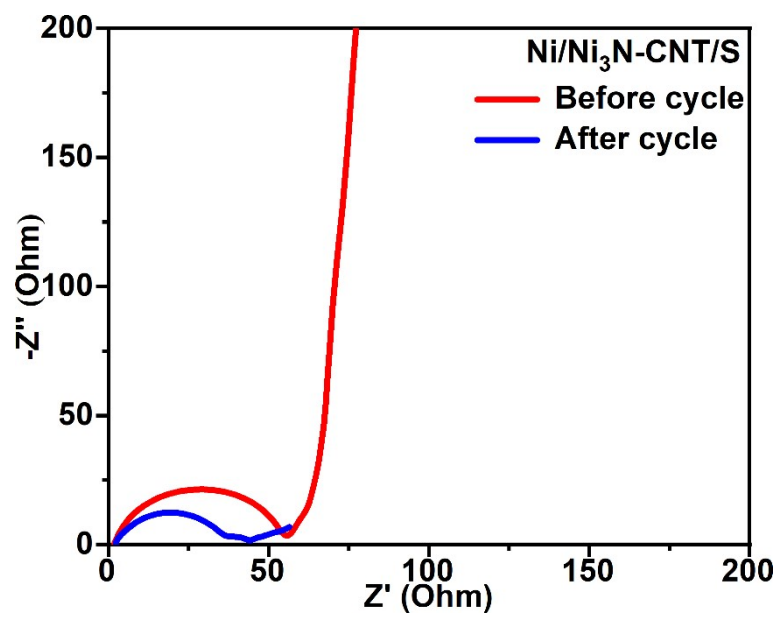


Figure S11. Nyquist plots of the Ni/Ni₃N-CNT/S electrode before and after cycling.

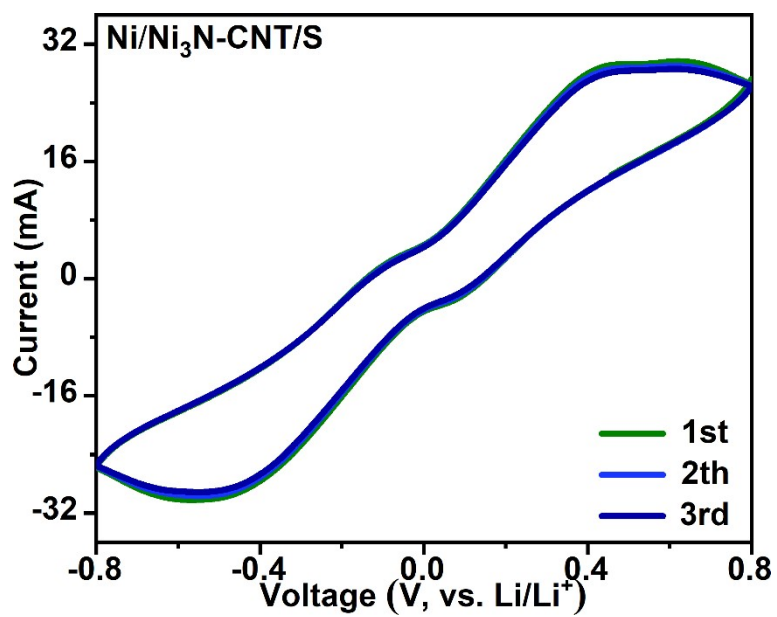


Figure S12. CV curves of Ni/Ni₃N-CNT and CNT symmetric cells in the first three cycle.

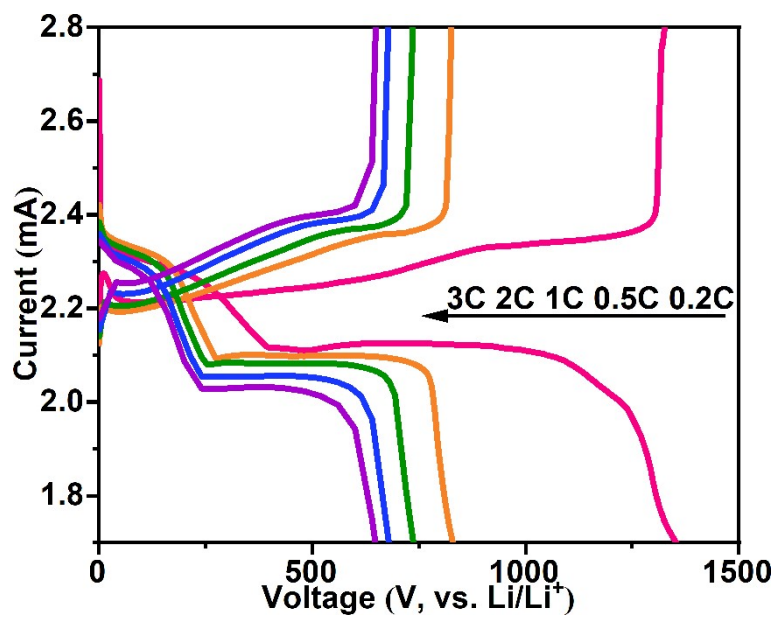


Figure S13. Galvanostatic charge-discharge curves of the Ni/Ni₃N-CNT/S electrode at 0.2-3 C.

References

1. W. Zhong, Q. W. Chen, F. Yang, W. Liu, G. D. Li, K. Xie and M. M. Ren, *J. Electroanal. Chem.*, 2019, **850**, 113392.
2. Z. Wu, S. Chen, L. Wang, Q. Deng, Z. Zeng, J. Wng and S. Deng, *Energy Stor. Mater.*, 2021, **38**, 381-388.
3. T. J. Xiao, L. X. Zhao, H. H. Ge, M. Z. Yang, W. L. Liu, G. D. Li, M. M. Ren, X. Zhang and Z. Zhou, *Chem. Eng. J.*, 2022, **439**, 1385-8947.
4. G. Kresse and J. Furthmüller, *Phys Rev B*, 1996, **54**, 11169-11186.
5. G. Kresse and D. Joubert, *Phys Rev B*, 1999, **59**, 1758-1775.
6. J. P. Perdew, K. Burke and M. Ernzerhof, *Phys Rev Lett*, 1996, **77**, 3865-3868.
7. B. Hammer, L. B. Hansen and J. K. Nørskov, *Phys Rev B*, 1999, **59**, 7413-7421.
8. H. J. Monkhorst and J. D. Pack, *Phys Rev B*, 1976, **13**, 5188-5192.